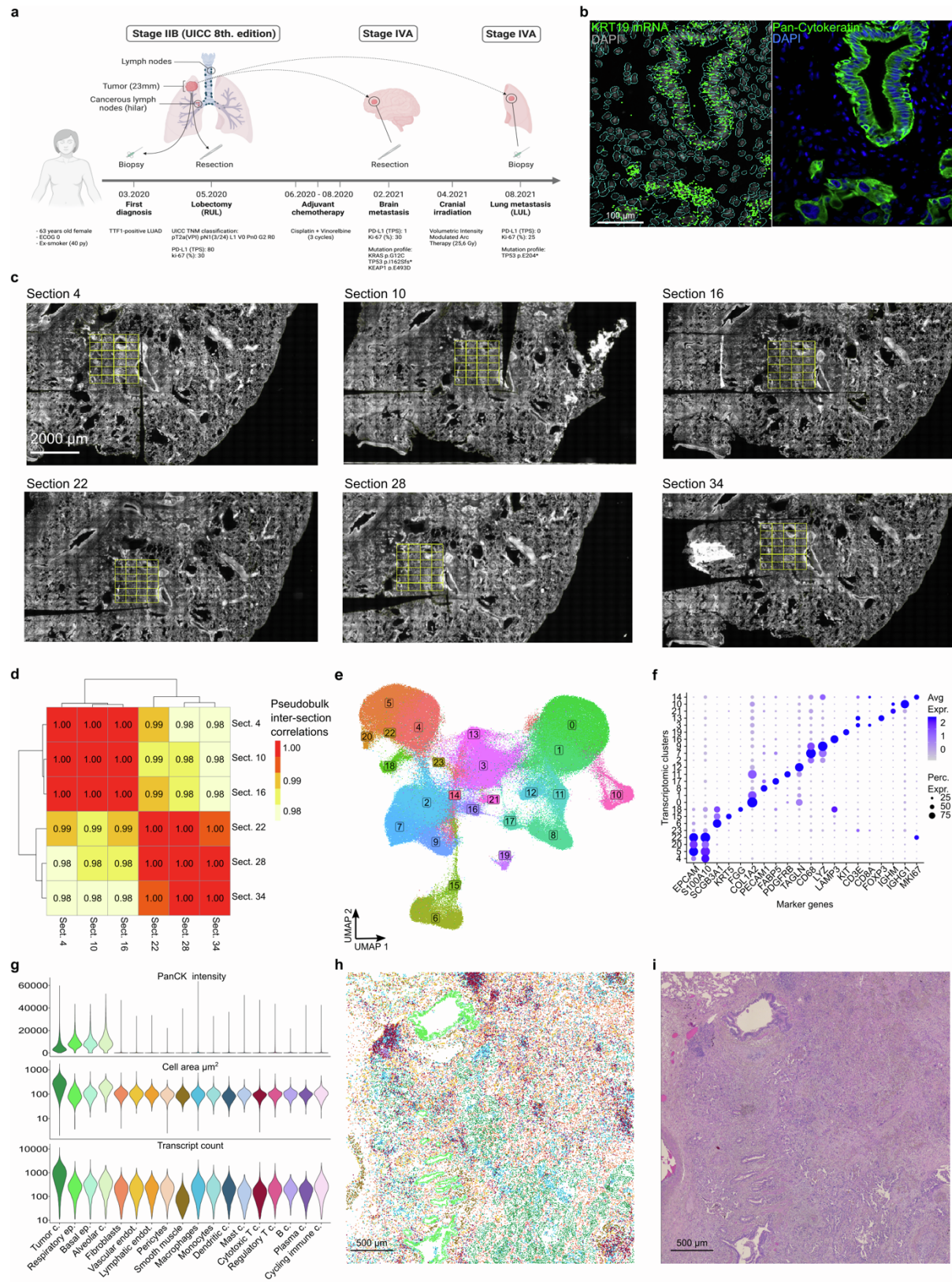


Supplemental information

Combining spatial transcriptomics and ECM imaging in 3D for mapping cellular interactions in the tumor microenvironment

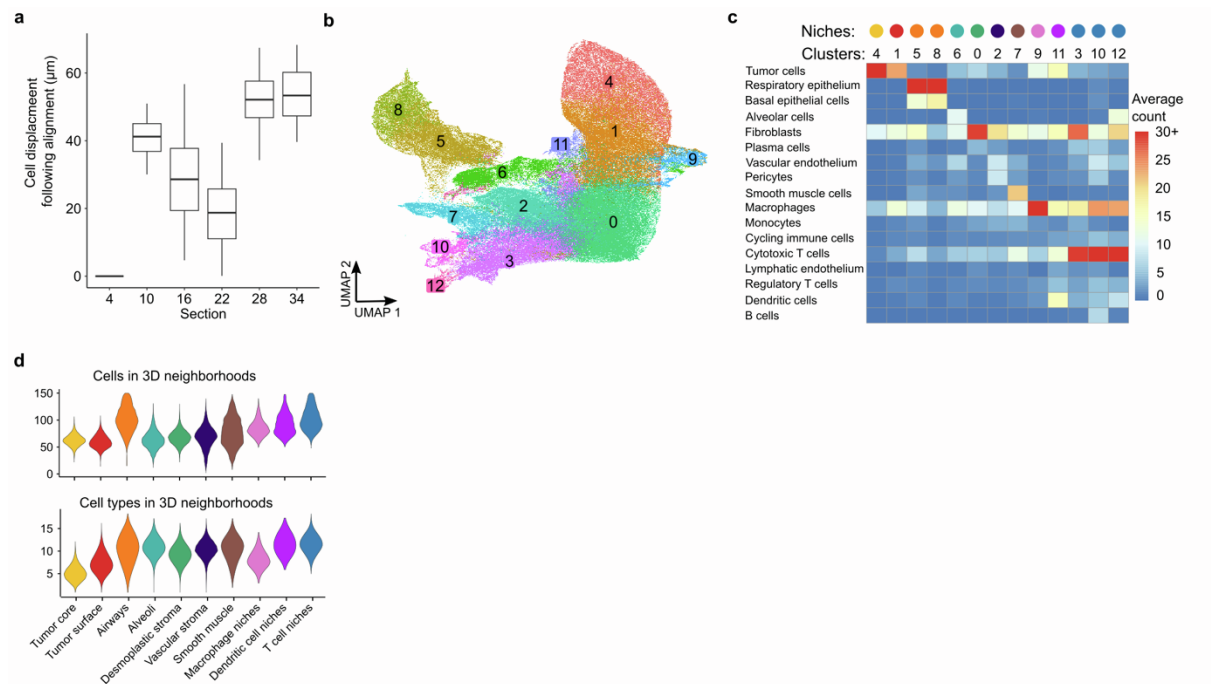
Tancredi Massimo Pentimalli, Simon Schallenberg, Daniel León-Periñán, Ivano Legnini, Ilan Theurillat, Gwendolin Thomas, Anastasiya Boltengagen, Sonja Fritzsche, Jose Nimo, Lukas Ruff, Gabriel Dernbach, Philipp Jurmeister, Sarah Murphy, Mark T. Gregory, Yan Liang, Michelangelo Cordenonsi, Stefano Piccolo, Fabian Coscia, Andrew Woehler, Nikos Karaiskos, Frederick Klauschen, and Nikolaus Rajewsky

SUPPLEMENTARY FIGURES

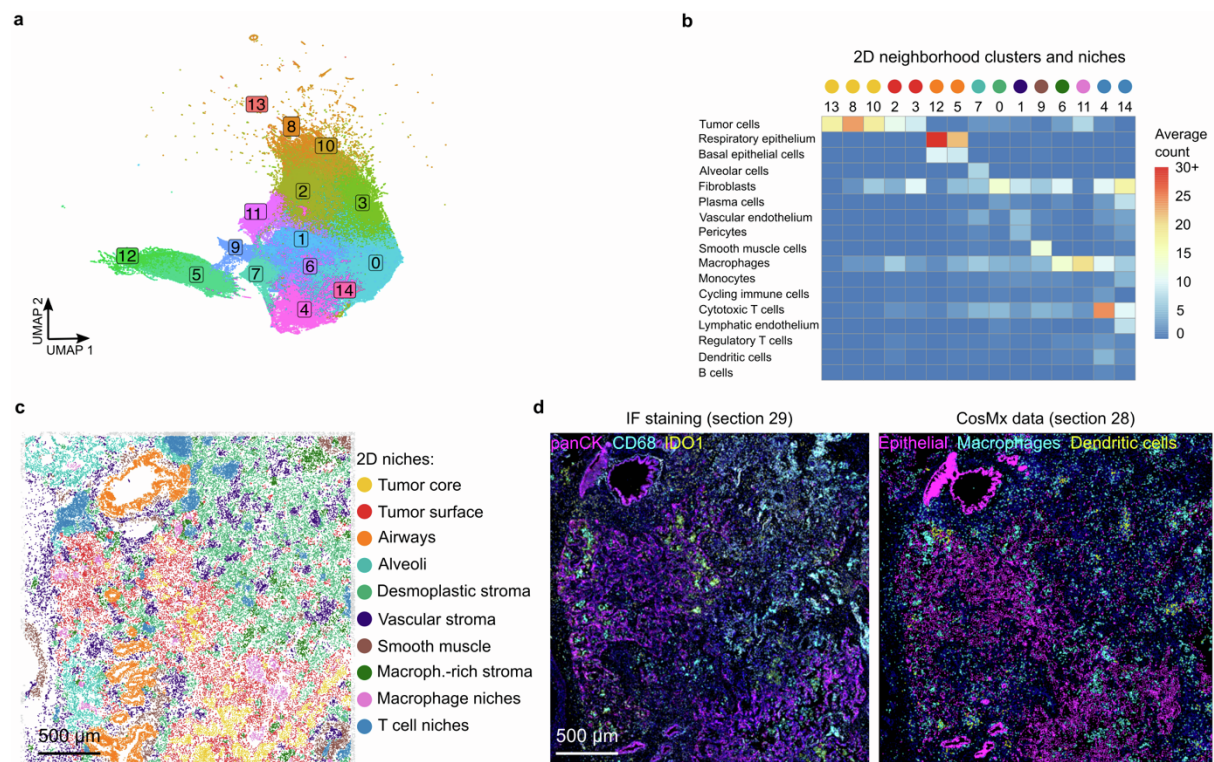


Supplementary figure 1, related to Figure 1. a) Schematics of characteristics, staging and

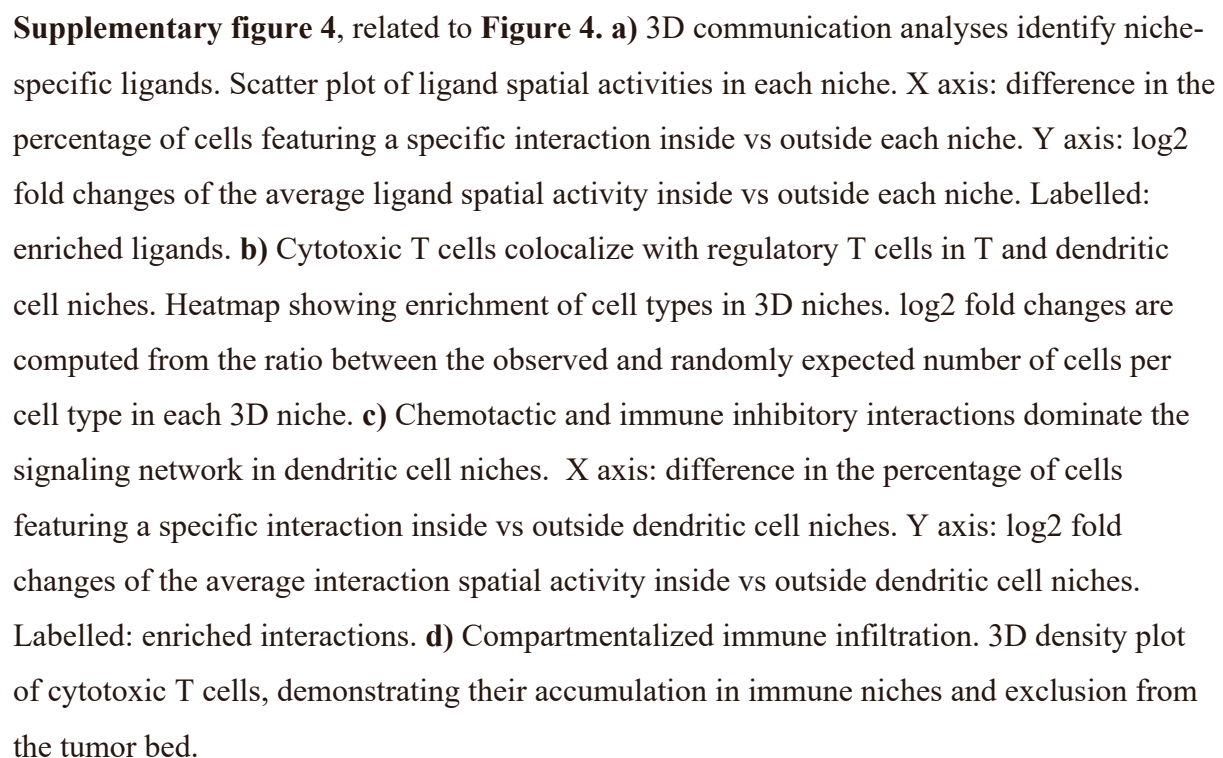
clinical history of the NSCLC patient under study. We investigated the lobectomy sample. **b)** Keratin 19 (KRT19) mRNA localization matches pan-cytokeratin immunostaining. Left: *KRT19* mRNA captured by CosMx (green: *KRT19* transcripts, gray: DAPI (nuclei), blue: cell segmentation masks). Right: pan-cytokeratin IF (epithelial cells, green; DAPI: blue). **c)** Whole slide images of the sections profiled with CosMx. Yellow: 24 fields of view in each ROI. **d)** Near-perfect correlation of gene expression across sections. Section-to-section Pearson correlation of aggregate gene expression profiles. **e)** UMAP of transcriptomic clusters. **f)** Cluster expression of canonical markers used for cell type annotations. **g)** Cell type distributions of pancytokeratin (panCK) immunofluorescence signal (top), segmentation mask area (middle) and transcript counts (bottom) per cell. **h)** Spatial plot of cell types in section 4. **i)** Tissue morphology by conventional hematoxylin and eosin staining in section 3.



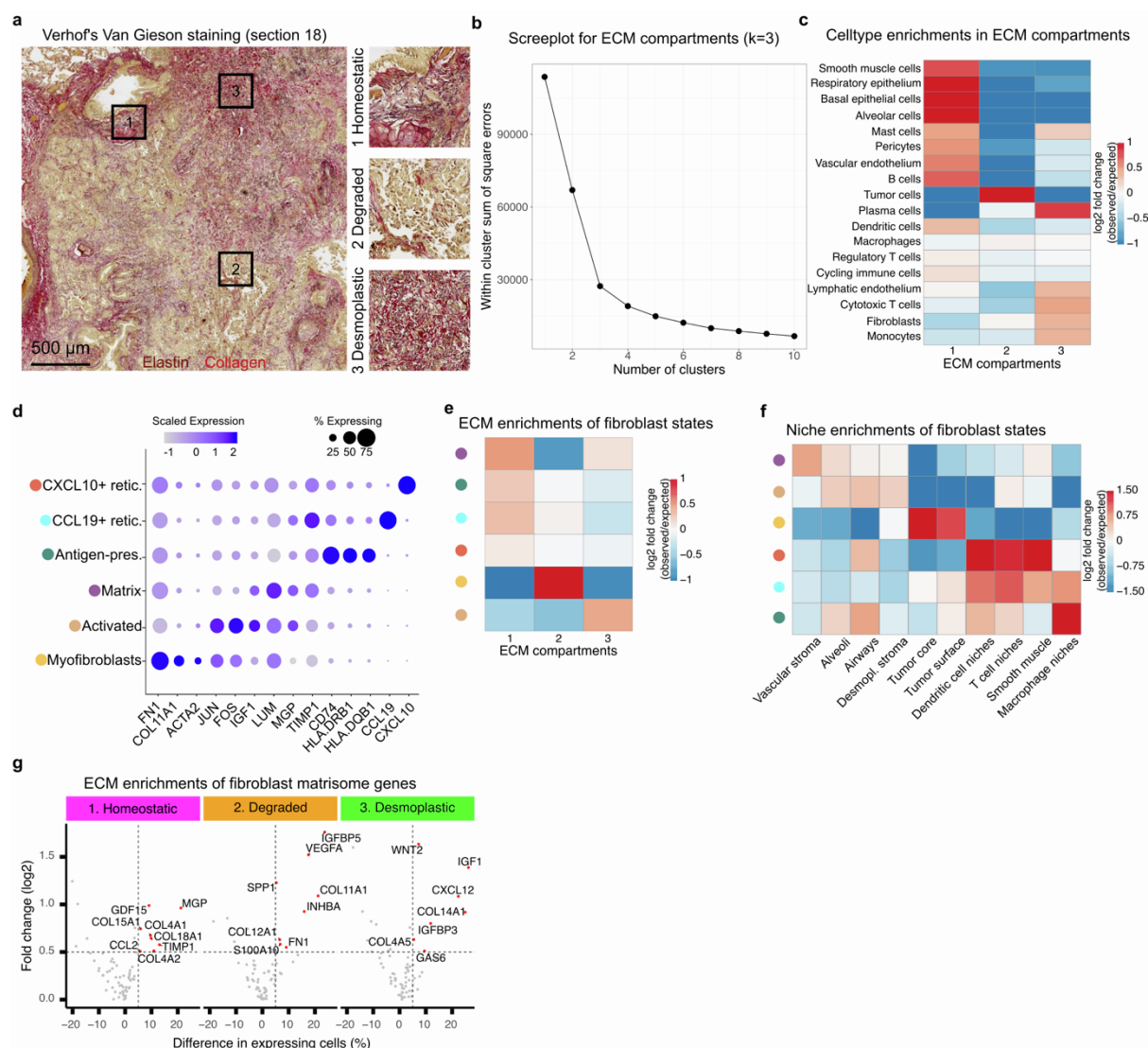
Supplementary figure 2, related to **Figure 2**. **a)** Impact of 3D alignment on cellular positions. Boxplot of cellular shifts of cells in each section following 3D alignment. Section 4 was used as the anchoring section. **b)** UMAP of 3D cellular neighborhoods clusters. **c)** Cell type composition of neighborhood clusters. Heatmap showing the average 3D neighborhood count of each cell type across neighborhood clusters. Heatmap legend is clipped to 30 for visualization purposes. Clusters with similar composition are merged in a single multicellular niche: Clusters 5 and 8 as ‘Airways’, cluster 3, 10 and 12 as ‘T cell niches’. Niche color legend in Fig 2c. **d)** Violin plots of the number of neighbors (top) and different cell types (bottom) per 3D neighborhood across 3D niches.



Supplementary figure 3, related to **Figure 3**. **a**) UMAP of 2D cellular neighborhoods clusters. **b**) Cell type composition of neighborhood clusters. Heatmap showing the average 2D neighborhood count of each cell type across neighborhood clusters. Heatmap legend is clipped to 30 for visualization purposes. Clusters with similar composition are merged in a single multicellular niche: Clusters 8, 10 and 13 as ‘Tumor core’, clusters 2 and 3 as ‘Tumor surface’, clusters 5 and 12 as ‘Airways’ and clusters 4 and 14 as ‘T cell niches’. **c**) Spatial map of 2D multicellular niches (section 10), gray: cells within 50 μ m of the section edge. **d**) Immunofluorescence validation of dendritic and macrophage niches. Left: Immunostaining (section 29) for nuclei (DAPI: blue) and tumor and normal epithelial cells (panCK: magenta), macrophages (CD68: cyan) and dendritic cells (ID01: yellow). Right: Spatial plot of celltypes (tumor and normal epithelial cells: magenta, macrophages: cyan, dendritic cells: yellow, others: blue) identified by CosMx in the adjacent section (section 28).

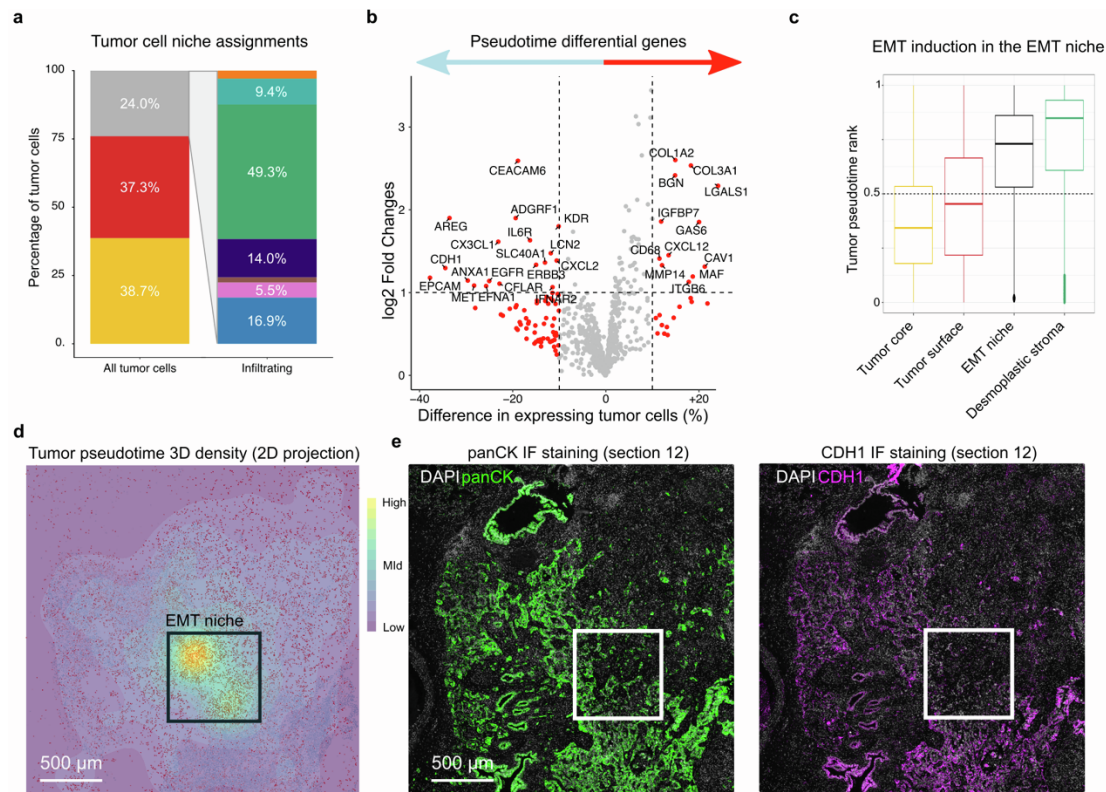


Supplementary figure 4, related to **Figure 4**. **a)** 3D communication analyses identify niche-specific ligands. Scatter plot of ligand spatial activities in each niche. X axis: difference in the percentage of cells featuring a specific interaction inside vs outside each niche. Y axis: log2 fold changes of the average ligand spatial activity inside vs outside each niche. Labelled: enriched ligands. **b)** Cytotoxic T cells colocalize with regulatory T cells in T and dendritic cell niches. Heatmap showing enrichment of cell types in 3D niches. log2 fold changes are computed from the ratio between the observed and randomly expected number of cells per cell type in each 3D niche. **c)** Chemotactic and immune inhibitory interactions dominate the signaling network in dendritic cell niches. X axis: difference in the percentage of cells featuring a specific interaction inside vs outside dendritic cell niches. Y axis: log2 fold changes of the average interaction spatial activity inside vs outside dendritic cell niches. Labelled: enriched interactions. **d)** Compartmentalized immune infiltration. 3D density plot of cytotoxic T cells, demonstrating their accumulation in immune niches and exclusion from the tumor bed.

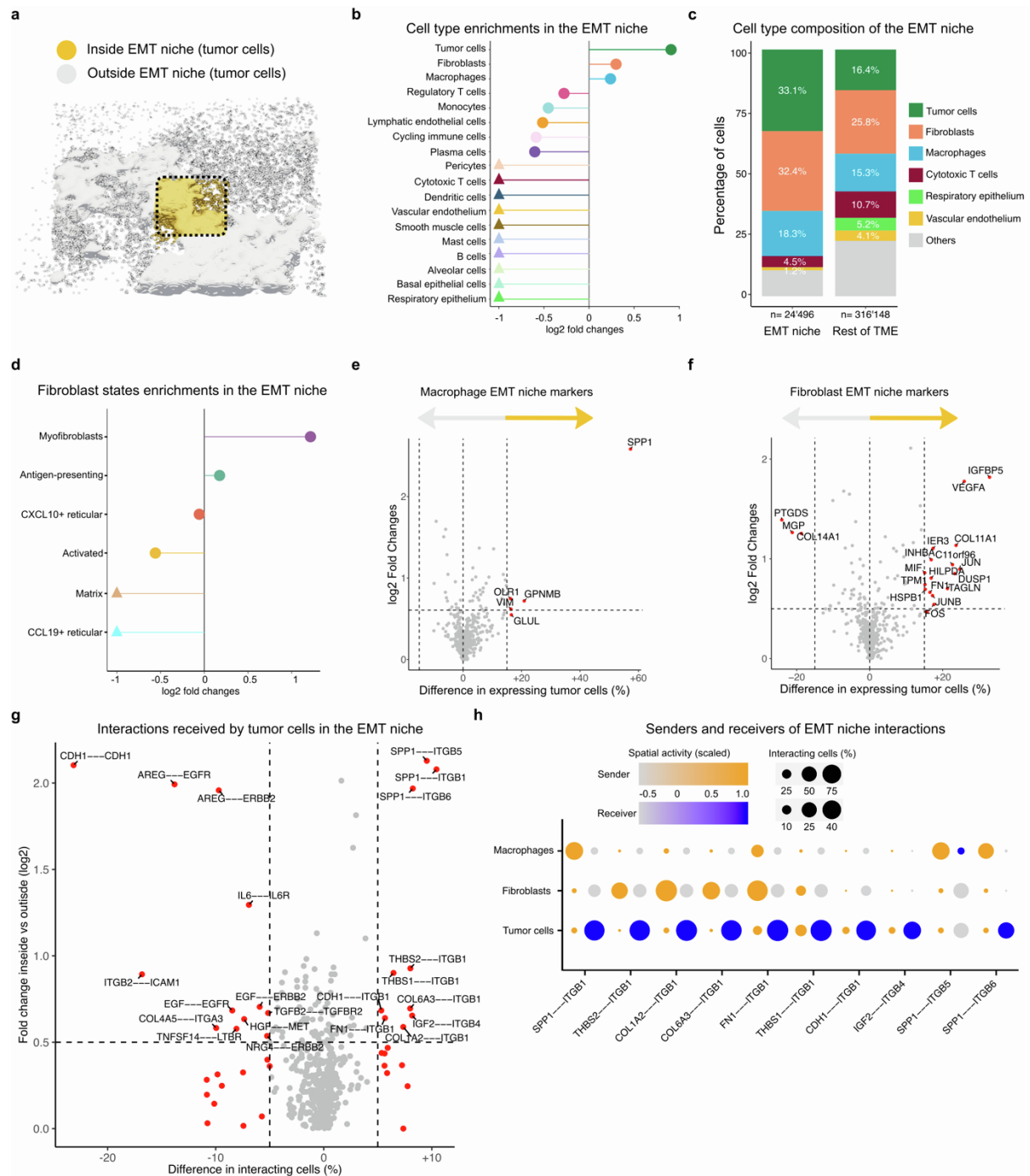


Supplementary figure 5, related to **Figure 5**. **a**) Verhoef's Van Gieson stain (section 18) validation of SHG imaging. Elastin (dark brown) and loose collagen fibers (red) characterize the homeostatic stroma (1), while the absence of elastin and thicker collagen bundles are found in the degraded (2) and desmoplastic (3) stroma, respectively. **b**) Heuristic identification of the optimal number of clusters for ECM compartments. Screeplot of k-means clustering of cellular neighborhood ECM composition. **c**) Cell types in the tumor microenvironment live in specific ECM compartments. Heatmap showing enrichment of cell types in ECM compartments. \log_2 fold changes are computed from the ratio between the observed and randomly expected number of cells per cell type in each 3D niche. **d**) Marker gene expression guides the annotation of fibroblast transcriptomic clusters. Dotplot of selected marker genes per fibroblast transcriptomic cluster. Dot size: percentage of cells expressing the gene. Dot color: scaled average expression. **e-f**) Fibroblast phenotypes are spatially linked with specific ECM compartments and multicellular niches. Heatmaps

showing enrichment of fibroblast phenotypes in ECM compartments (e) and multicellular niches (f). log2 fold changes are computed from the ratio between the observed and randomly expected number of cells per fibroblast phenotype. **g)** The integrative analysis of ECM composition and fibroblast gene expression identifies matrisome genes enriched in ECM compartments. Scatter plot of matrisome gene expression in each niche. X axis: difference in the percentage of fibroblasts expressing a specific matrisome gene inside vs outside each ECM compartment. Y axis: log2 fold changes of the average SCT-normalized fibroblast gene expression inside vs outside each ECM compartment. Labelled: enriched matrisome genes.



Supplementary figure 6, related to **Figure 6**. **a**) 3D neighborhoods enable the study of infiltrating tumor cells. Tumor cells assignment to multicellular niches identifies infiltrating tumor cells. Stacked barplots of all tumor cells (left) and infiltrating tumor cells (right) assignments to multicellular niches (yellow: tumor core, red: tumor surface, gray: outside the tumor bed, further color legend in Fig2c). **b**) Epithelial-to-mesenchymal transition (EMT) genes drive tumor pseudotime. Scatter plot of differential gene expression in tumor cells with late (rank > 0.5, right) vs early (rank \leq 0.5, left) pseudotime. X axis: difference in the percentage of expressing tumor cells with late vs early pseudotime. Y axis: log2 fold changes of the average SCT-normalized tumor gene expression. Red: genes with more > 5% expression difference labelled: pseudotime enriched genes. **c**) Tumor EMT is induced in the EMT niche and desmoplastic stroma. Boxplot of pseudotime rank in tumor cell neighborhoods across the EMT niche and the rest of the tumor bed and desmoplastic stroma. **d**) Mesenchymal tumor cells density peaks in the EMT niche (black box). 3D spatial density of tumor cells with late pseudotime (rank > 0.75). **e**) Immunofluorescence validation of CDH1 downregulation in the EMT niche (section 12). Left: Immunostaining for nuclei (DAPI: white) and tumor and normal epithelial cells (panCK: green). Right: Immunostaining for nuclei (DAPI: white) and epithelial phenotype (CDH1: magenta), white square: EMT niche.



Supplementary figure 7, related to **Figure 7**. **a**) The EMT niche is located at the interface between tumor surface and the surrounding stroma. 3D rendering of EMT niche (yellow), the tumor bed and infiltrating tumor cells (gray). **b**) Tumor cells, fibroblasts and macrophages are the only cell types enriched in the EMT niche. log2 fold changes are computed from the ratio between the observed and expected number of cells per cell type in the EMT niche. **c**) Evidence of EMT niche cellular remodeling. Stacked barplot of cell type assignment in the EMT niche (left) and the rest of the tumor microenvironment (right). Gray: cell types with <4% abundance in both regions. **d**) Myofibroblasts are enriched in the EMT niche. log2 fold

changes are computed from the ratio between the observed and expected number of cells per fibroblast phenotype in the EMT niche. **e)** SPP1, M2 and lipid-laden markers identify macrophages in the EMT niche. Scatter plot of differential gene expression in macrophages inside vs outside the EMT niche. X axis: difference in the percentage of expressing macrophages. Y axis: log2 fold changes of the average SCT-normalized macrophage gene expression. Labelled: EMT niche differential macrophage genes. **f)** VEGFA and IGFBP5 expression marks fibroblasts in the EMT niche. Scatter plot of differential gene expression in fibroblasts inside vs outside the EMT niche. X axis: difference in the percentage of expressing fibroblasts. Y axis: log2 fold changes of the average SCT-normalized fibroblasts gene expression. Labelled: EMT niche differential fibroblast genes. **g)** Integrin interactions dominate the signaling network in the EMT niche. X axis: difference in the percentage of tumor cells receiving a specific interaction inside vs outside the EMT niche. Y axis: log2 fold changes of the average interaction spatial activity inside vs outside the EMT niche. Labelled: differential interactions. **h)** Fibroblasts and macrophages stimulate tumor integrin signaling in the EMT niche. Dotplot of receptor-ligand interactions enriched in the EMT niche. Dot size: cell type-specific percentage of sender and recipient cells, dot color: cell type-specific scaled average interaction score as ligand sender (orange) and receptor receiver (blue).